Entanglement dynamics in the Lipkin-Meshkov-Glick model

Julien Vidal,[1] Guillaume Palacios,[1] and Claude Aslangul[1]
[1]*Groupe de Physique des Solides, CNRS UMR 7588, Campus Boucicaut, 140 rue de Lourmel, 75015 Paris, France*
(Received 21 June 2004; published 3 December 2004)

The dynamics of the one-tangle and the concurrence is analyzed in the Lipkin-Meshkov-Glick model which describes many physical systems such as the two-mode Bose-Einstein condensates. We consider two different initial states which are physically relevant and show that their entanglement dynamics are very different. A semiclassical analysis is used to compute the one-tangle which measures the entanglement of one spin with all the others, whereas the frozen-spin approximation allows us to compute the concurrence using its mapping onto the spin squeezing parameter.

DOI: 10.1103/PhysRevA.70.062304 PACS number(s): 03.67.Mn, 03.65.Ud, 73.43.Nq

I. INTRODUCTION

In recent years, the interplay between entanglement and quantum phase transitions has been the subject of many studies. Since the pioneering works on the Ising model in a transverse magnetic field [1,2] exhibiting the key role played by entanglement in quantum critical phenomena, lots of effort have been devoted to characterize the intricate structure of the ground state in spin systems [3–22] as well as in electron models [23–25]. All these studies show that entanglement, a genuine quantum property, can be used to probe the phase diagram of a system and especially to detect quantum phase transitions. Unfortunately, such analyses are often restricted to one-dimensional (1D) systems where exact solutions exist and allow one to deal with the thermodynamical limit. Usually, higher-dimensional systems require a numerical treatment which is limited by the Hilbert space dimension which grows exponentially with the number of degrees of freedom. However, when the Hamiltonian has a large symmetry group as is here the case, it is still possible to study the large-N limit.

In the present paper, we consider N mutually interacting spins $1/2$ embedded in a magnetic field. The restriction of this model to the fully symmetric subspace can be mapped, via the Schwinger representation, onto interacting bosons in a two-level system coupled by a tunneling term. Thus, although it has initially been introduced by Lipkin, Meshkov, and Glick (LMG) [26–28] in nuclear physics, this model is also relevant to describe the Josephson effect or two-mode Bose-Einstein condensate (BEC). This ubiquity in very different domains is certainly one of the reason why it has been periodically rediscovered (see, for example, Refs. [29–31]). Its integrability has even recently been proven in a series of papers (see Ref. [32] for a review) and a complete solution has been derived using the algebraic Bethe ansatz [33]. The ground-state entanglement properties of this model have been analyzed for both ferromagnetic [34,35] and antiferromagnetic coupling [36] using the concurrence [37] (see below for details). Here, our goal is to analyze the entanglement dynamics which has, so far, been mostly investigated in 1D spin systems [38,39].

The possibility of experiments in BEC's has led several groups to study the dynamics in the LMG model but entanglement has been discussed only recently [40–43]. In this study, we investigate the time evolution of two peculiar states which are relevant in the BEC context since they correspond to situations where all atoms are either in one of the two modes or equally distributed between both modes. For these two states, we discuss the entanglement dynamics through two observables: namely, the one-tangle which measures the entanglement of one spin with all others and the concurrence which quantifies the two-spin entanglement. In the next section, we introduce the LMG model and discuss its phase diagram. In Sec. III, we define the entanglement measures used throughout this paper and give several canonical examples. The ground-state entanglement properties [34–36] are briefly recalled in Sec. IV. The quantum dynamics is presented in Sec. V for the two states mentioned above. We show that the one-tangle and the concurrence have completely different behaviors depending on the initial state. These characteristics can be understood in several limiting cases that we discuss in detail.

II. THE LIPKIN-MESHKOV-GLICK MODEL

We consider a system of mutually interacting spins $1/2$ embedded in a magnetic field described by the following Hamiltonian introduced by LMG [26–28] in a more general form:

$$H = -\frac{\lambda}{N}\sum_{i<j} \sigma_x^i \sigma_x^j - h\sum_i \sigma_z^i \tag{1}$$

$$= -\frac{2\lambda}{N}S_x^2 - 2hS_z + \frac{\lambda}{2}, \tag{2}$$

where the σ_α's are the Pauli matrices and $S_\alpha = \Sigma_i \sigma_\alpha^i/2$. The prefactor $1/N$ is necessary to get a finite free energy per spin in the thermodynamical limit. The Hamiltonian H preserves the magnitude of the total spin and does not couple states having a different parity of the number of spins pointing in the magnetic field direction (spin-flip symmetry): namely,

$$[H, \mathbf{S}^2] = 0, \tag{3}$$

$$\left[H, \prod_i \sigma_z^i\right] = 0. \tag{4}$$

The phase diagram of this model can be easily derived using a semiclassical description [30]. For a ferromagnetic coupling ($\lambda > 0$), the system undergoes a second-order quantum phase transition at the critical field $h_c = \lambda$, whereas for antiferromagnetic interactions, a first-order quantum phase transition occurs at zero field.

III. ENTANGLEMENT MEASURES

To analyze the entanglement dynamics, we focus here on two commonly used quantities: the one-tangle which measures the entanglement of one spin with the others and the concurrence which measures the two-spin entanglement. For a given pure state $|\psi\rangle$, both quantities are computed from the density matrix $\rho = |\psi\rangle\langle\psi|$.

The one-tangle is defined as follows:

$$\tau_i = 4 \det \rho_i^{(1)} = 1 - \sum_\alpha \langle \sigma_\alpha^i \rangle^2, \tag{5}$$

where $\rho_i^{(1)}$ is the one-spin reduced density matrix obtained from ρ by tracing out over all spins except spin i and where $\langle A \rangle = \mathrm{Tr}[\rho_i^{(1)} A]$. The one-tangle τ_i ranges between 0 and 1. It vanishes for a state such that $|\psi\rangle = |\phi\rangle_i \otimes |\varphi\rangle$ and reaches 1 for maximally entangled states such as the famous Einstein-Podolsky-Rosen (EPR) state [44]

$$|\mathrm{EPR}\rangle = \frac{1}{\sqrt{2}}(|\uparrow\downarrow\rangle - |\downarrow\uparrow\rangle). \tag{6}$$

To measure the two-spin entanglement, we consider the concurrence C introduced by Wootters [37]. This quantity is computed from the two-spin reduced density matrix $\rho_{i,j}$ obtained by tracing out ρ over all spins except spins i and j. Next, we introduce the spin-flipped density matrix $\tilde{\rho}_{i,j} = \sigma_y \otimes \sigma_y \rho_{i,j}^* \sigma_y \otimes \sigma_y$ where $\rho_{i,j}^*$ is the complex conjugate of $\rho_{i,j}$. The concurrence C is then defined by

$$C_{i,j} = \max\{0, \mu_1 - \mu_2 - \mu_3 - \mu_4\} \equiv \max\{0, C_{i,j}^*\}, \tag{7}$$

where the μ_k's are the square roots of the four real eigenvalues of $\rho_{i,j}\tilde{\rho}_{i,j}$ and where $\mu_i \geqslant \mu_{i+1}$. The concurrence vanishes, for example, for any state $|\psi\rangle = |\chi\rangle_i \otimes |\phi\rangle_j \otimes |\varphi\rangle$ and reaches its maximum value $C=1$ for states such as $|\mathrm{EPR}\rangle$.

Let us also mention that τ and C are related through the Coffman-Kundu-Wootters (CKW) conjecture [45] stating that

$$\tau_i \geqslant \sum_{j \neq i} C_{i,j}^2. \tag{8}$$

Note that for pure two-spin states, we have an exact equality. In the present study, we have systematically checked that this conjecture (8) was always verified.

Finally, we would like to stress that tracing out the density matrix ρ can induce or destroy some correlations between spins. For instance, a nonseparable state, such as the Greenberger-Horne-Zeilinger (GHZ) state [46]

$$|\mathrm{GHZ}\rangle = |\psi\rangle = \frac{1}{\sqrt{2}}(|\uparrow\uparrow\uparrow\rangle + |\downarrow\downarrow\downarrow\rangle), \tag{9}$$

has a maximum one-tangle ($\tau=1$) and a vanishing concurrence ($C=0$). It is thus important to keep in mind that these measures only give partial information about the entanglement of the state.

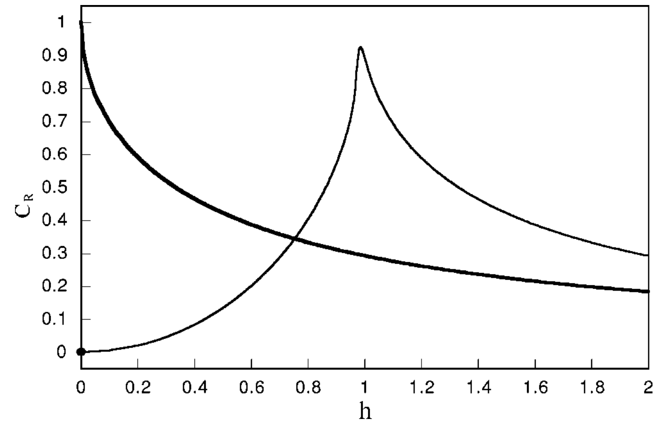

FIG. 1. Rescaled concurrence of the ground state for $\lambda = +1$ (thin line) and $\lambda = -1$ (thick line) ($N = 10^3$ spins). In both cases, $C_R = 0$ for $h = 0$.

IV. GROUND-STATE ENTANGLEMENT

We recall in this section the main features of the ground-state entanglement and we refer the reader to Refs. [34–36] for a detailed discussion.

As explained in Sec. II, the ground state of H is well described by a mean-field approach showing that in the thermodynamical limit the ground state is given by a product state [30] for which $\tau = C = 0$. However, in the symmetric phase ($\lambda > 0$ and $h < \lambda$), we underline that the ground state is twofold degenerate in the thermodynamical limit, whereas at finite N, it is unique (except for $h=0$). In the degenerate case, one must consider the thermal density matrix at zero temperature [34] to compute the entanglement properties. This implies in particular that the one-tangle in this phase is given by $\tau = 1 - (h/\lambda)^2$ and that $C=0$ in the large-N limit. However, the finite-N corrections to this separable asymptotic form allow one to capture a nontrivial behavior of the rescaled concurrence $C_R = (N-1)C$. This rescaling is actually the coordination number of each site and takes into account the fact that the two-site entanglement, as measured by the concurrence, is, in this model, equally shared between all sites.

For a ferromagnetic coupling ($\lambda > 0$), C_R displays a cusp-like behavior at the critical point $h_c = \lambda$ (see Fig. 1) where C_R goes to 1 in the thermodynamical limit.

In the antiferromagnetic case, C_R is a smoothly decreasing function of h but is discontinuous at $h=0$ where a first-order transition occurs (see Fig. 1). For $h=0^+$, C_R reaches 1 in the thermodynamical limit, but for $h=0$, the ground state is given by zero total spin states for which $C_R=0$.

Except for this very special point, the ground state always lies in the maximum spin sector $S=N/2$ for any λ. Moreover, at finite N and in the large-field limit, the ground state is the fully polarized state in the z direction,

$$|\psi_0\rangle = |Z\rangle = \otimes_{i=1}^{N} |\uparrow\rangle, \qquad (10)$$

for which one also has $C_R=0$.

In the antiferromagnetic case, the entanglement properties of the ground state (restricted to the maximum spin sector $S=N/2$) have also been analyzed by Hines *et al.* [40] through the von Neumann entropy $E(h)$ for bipartite systems. In BEC language, the two subsystems correspond to the two components of the condensate—i.e., to the states polarized in the $\pm x$ direction. This quantity has thus nothing to do with the concurrence and its behavior is indeed very different: E vanishes for $h=0$ (since $|\psi_0\rangle=|X\rangle$) whereas C_R is maximum (in this spin sector) and E is maximum in the large-field limit whereas C_R vanishes.

More recently, another entropy $S(h)$ has been analyzed in the LMG model [47]. This entropy is based on a bipartite decomposition in two subsytems of size L and $N-L$. Here $S(h)$ has been found to be maximum at the critical point h_c in agreement with a recent conjecture proposed by Hines *et al.* [48]. Moreover, a logarithmic scaling has been observed and may reveal an underlying 1D conformal field theory [47] for the LMG model.

V. QUANTUM DYNAMICS

In this section, we analyze the quantum dynamics of two initial states belonging to the maximum spin subspace $S=N/2$: (i) the state $|X\rangle$ fully polarized in the x direction which corresponds, in BEC language, to a state where the atoms are all localized in one of the two modes and (ii) the state $|Z\rangle$ fully polarized in the z direction which corresponds, in BEC language, to a state where the atoms are equally distributed between both modes (catlike state).

The quantum dynamics of these two states have already been widely studied for this model in the BEC context [40,41,49–54]. Here, we focus on the entanglement dynamics by studying the time evolution of $\tau(h,t)$ and $C_R(h,t)$, which do not depend on the spins kept in the trace operation since states belonging to the subspace $S=N/2$ are invariant under the permutation group. This implies in particular that τ and C_R only depend on the magnetization $\langle S_\alpha\rangle$ and on the correlation functions $\langle S_\alpha S_\beta\rangle$ [55].

A. Time scales

As explained in Ref. [56], the spectrum of H remains discrete in the thermodynamical limit; i.e., the mean level spacing remains finite when N goes to infinity. For equidistant levels, we would expect to have a Poincaré time that does not depend on N. However, it turns out that the Poincaré time scales here linearly with N. As noticed by Milburn *et al.* [54], the semiclassical dynamics (see below) mimics very well the quantum dynamics up to a given time scale t_{sc}, which is of the order of the Poincaré time. For times smaller than t_{sc}, the system thus remains nonentangled, and in the large-N limit, it is described by the classical equations of motion (see Appendix B). For times larger than t_{sc} quantum effects become important, some revivals of the wave-packet are observed, and the latter approach fails. It is thus in this regime that interesting and nontrivial entanglement properties must be analyzed. Consequently, we always consider a dimensionless rescaled time $\mu=4\lambda t/N$ which allows us to investigate the dynamics and to easily compare the results for various N. Of course, we have checked in each situation that the time-averaged results were weakly sensitive to the time range chosen provided this latter was sufficiently large.

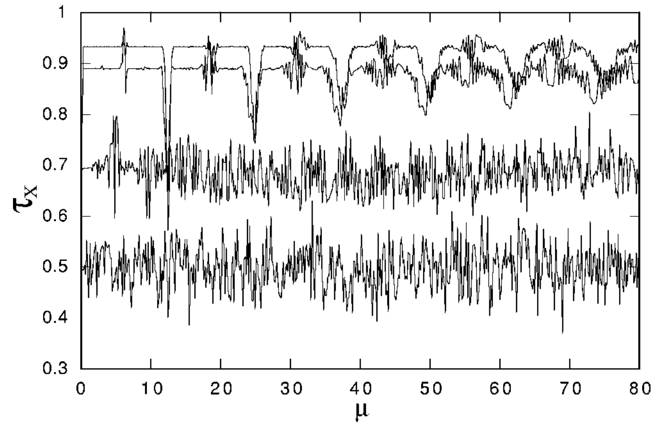

FIG. 2. Behavior of τ_X as a function of $\mu=4\lambda t/N$ for different values of the field $h=0.5$, 0.55, 0.8, 1 from bottom to top ($\lambda=+1$ and $N=10^3$).

We must also mention recent studies [52,53] which reveal multiple time scales in the LMG model (called the boson-Hubbard dimer model in these papers). However, the range of validity of these results is confined to $h \ll \lambda/N$ (small-tunneling-amplitude regime in boson language) which is not the regime considered here. Yet we cannot exclude larger characteristic time scales but such a study is beyond the scope of the present paper and we shall leave this question apart in the following.

B. $|X\rangle$ state

It is clear that the entanglement properties of the $|X\rangle$ state are insensitive to the transformation $h \leftrightarrow -h$. Thus, as explained in Appendix A, one can, in this case, restrict our analysis to $\lambda \geqslant 0$ and $h \geqslant 0$.

(i) For $h=0$, the $|X\rangle$ state is an eigenstate of H so that $\tau_X(h=0)=0$ and $C_X(h=0)=0$ for all time t.

(ii) For $\lambda=0$, H is completely separable and thus both τ_X and C_X vanish. However, for this state, this limit is highly singular since, for any finite coupling λ, the large-field limit leads to nontrivial entanglement properties ($\tau_X \to 1$) as can be seen in Fig. 2.

Apart from these limiting cases, we have been unable to get analytical expressions of the one-tangle for this state. We have displayed in Figs. 2 and 3 the behavior of τ_X for different values of the magnetic field as a function of μ.

For $h \ll \lambda$, the characteristic energy scale driving the dynamics is λ/N and hence τ is almost periodic in μ with period 2π [Fig. 3 (bottom)]. In this regime, quantum fluctuations are weak and τ is a smooth function of μ. When μ increases, the depth of the hollows which corresponds to a

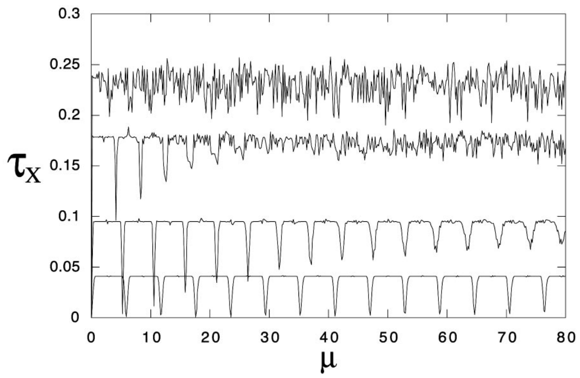

FIG. 3. Same as Fig. 2 for h=0.2, 0.3, 0.4, 0.45 from bottom to top.

revival of the wave packet decreases and eventually goes to zero in the large μ limit so that, in this limit, τ_X is almost constant. When h increases, quantum fluctuations become more and more important and τ_X becomes more and more "noisy." The maximum of these fluctuations is reached for $h=\lambda/2$ which corresponds to the critical field of the semiclassical dynamics [41,54]. Below (above) this critical field, $\langle S_x \rangle$ (which represents the difference of population between the two wells in the BEC problem) oscillates around a nonvanishing (vanishing) value. In the other limit $h \gg \lambda$, where the magnetic field dominates, τ_X goes to 1 and displays a pseudoperiodic behavior in μ with period 4π as can already be inferred for $h=\lambda$ in Fig. 2 (top). At large times, the depth of the cusplike behavior present for $\mu=0[4\pi]$ decreases and τ is also almost constant. To go beyond this qualitative description, we have computed the time-averaged value of the one-tangle $\overline{\tau_X}$ as a function of h. As shown in Fig. 4, the large N limit of $\overline{\tau_X}$ can be partially captured by a simple semiclassical approach, especially when quantum fluctuations are weak—i.e., far from $h=\lambda/2$.

For a detailed discussion of this approach, we refer the reader to Refs. [41,54]. The main idea is to compute the solution of the semiclassical equations for the quantity S_α.

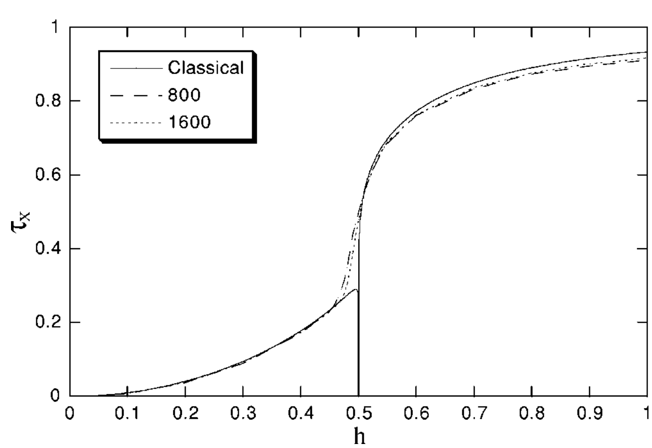

FIG. 4. Time-averaged value of τ_X as a function of the magnetic field h for N=800, 1600 ($\lambda=+1$). The solid line is obtained from the "(semi) classical time-averaged one-tangle" as explained in the text.

For an initial state polarized in the x direction, these equations can be exactly solved following Eilbeck *et al.* [57] and one gets

$$S_x^{sc}(t) = \frac{N}{2}\mathrm{cn}(2ht|k^2), \tag{11}$$

$$S_y^{sc}(t) = -\frac{N}{2}\mathrm{dn}(2ht|k^2)\mathrm{sn}(2ht|k^2), \tag{12}$$

$$S_z^{sc}(t) = \frac{N\lambda}{4h}\mathrm{sn}^2(2ht|k^2), \tag{13}$$

where cn, dn, and sn are the Jacobi elliptic functions and where $k=\lambda/2h$ (see Appendix B for details). These S_α^{sc}'s are periodic functions with a period $2K(k^2)/h$ for $k^2<1$ and $2K(k^2)/\lambda$ for $k^2>1$ where K denotes a complete elliptic integral of the first kind. Note that the case $k^2=1$ is singular since the upper and lower limits do not coincide.

Of course, if we compute the one-tangle using these semiclassical expressions, we trivially find

$$\tau_X^{sc} = 1 - \frac{4}{N^2}\sum_\alpha (S_\alpha^{sc})^2 = 0 \tag{14}$$

and, consequently, $\overline{\tau_X^{sc}}=0$ for all h. However, as said above, the fluctuations of τ_X are pretty weak at least away from $h=\lambda/2$. Thus, assuming that τ_X is constant, we replace $\overline{\langle S_\alpha\rangle^2}$ by $(\overline{S_\alpha^{sc}})^2$:

$$\overline{\tau_X} = 1 - \frac{4}{N^2}\sum_\alpha \overline{\langle S_\alpha\rangle^2} \simeq 1 - \frac{4}{N^2}\sum_\alpha (\overline{S_\alpha^{sc}})^2. \tag{15}$$

Obviously, this crude approximation is to be justified only for constant $\langle S_\alpha\rangle$ and S_α^{sc}, provided the semiclassical description is meaningful—i.e., in the large-N limit. After time-averaging the S_α^{sc}'s over one period, we thus get a "semiclassical time-averaged one-tangle." This quantity is depicted in Fig. 4, and as expected it is in excellent agreement away from $h=\lambda/2$. Near this point, since the quantum fluctuations are very strong, the approximation (15) fails and the discrepancy is large. In the large-field limit, one has $\overline{S_\alpha^{sc}}=0$ for all α and thus $\overline{\tau_X}=1$.

Let us now discuss the concurrence dynamics for the $|X\rangle$ state whose behavior is depicted in Figs. 5 and 6 for different values of the magnetic field. At small field [$h<\lambda/2$ (see Fig. 5)], $C_{X,R}^*$ is most often negative but displays some peaks (where $C_{X,R}^*>0$) which coincides with the hollows in τ_X and whose amplitude goes to zero when μ increases. As a result, at large times, the rescaled concurrence $C_{X,R}$ always vanishes. When h increases, this phenomenon is amplified and, as for the one-tangle, $C_{X,R}^*$ fluctuates more and more until $h=\lambda/2$ where it reaches its minimum value. Above this critical field, $C_{X,R}^*$ increases when h increases, but remains always negative at large times. Note that at short times there is, for any h, a "peak of concurrence" for which $C_{X,R}^*$ is positive, but as time goes on, it is always negative.

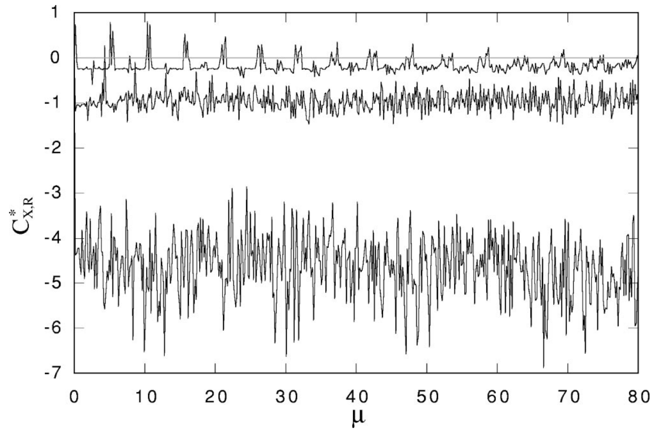

FIG. 5. Behavior of $C^*_{X,R}$ as a function of $\mu=4\lambda t/N$ for different values of the field $h=0.3$, 0.4, 0.45 from top to bottom ($\lambda=+1$ and $N=10^3$). The grey line corresponds to the threshold $C=0$.

To summarize, at sufficiently large times and for any values of the magnetic field h, the rescaled concurrence $C_{X,R}$ always vanishes.

C. $|Z\rangle$ state

The $|Z\rangle$ state is an eigenstate of the operator $\Pi_i\sigma_z^i$ which commutes with H. As a consequence, at all times, one has $\langle S_x\rangle=\langle S_y\rangle=0$, so that

$$\tau_Z = 1 - \frac{4}{N^2}\langle S_z\rangle^2. \tag{16}$$

In addition and contrary to the $|X\rangle$ state, it is obvious that the direction of the magnetic field h plays a role in the dynamics of $|Z\rangle$. Thus, to investigate all possible situations, we consider the case $\lambda \geqslant 0$ for all h, the region $\lambda<0$ being obtained by transformations discussed in Appendix A.

(i) For $h=0$, H is trivially solvable as well as the time evolution of the $|Z\rangle$ state. As detailed in Ref. [55], one finds, in this case,

$$\tau_Z(h=0,t) = 1 - \cos(\mu/2)^{2(N-1)}, \tag{17}$$

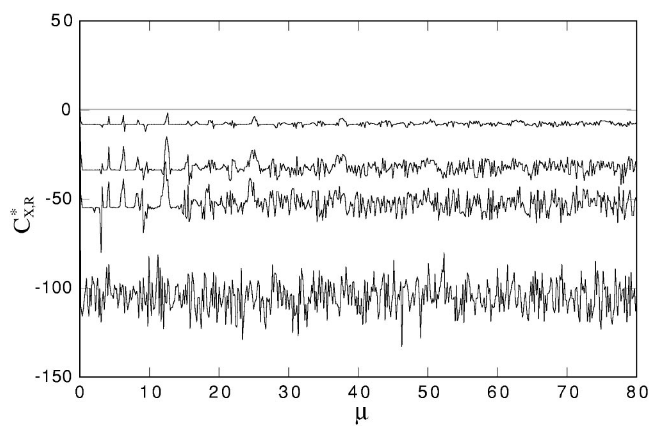

FIG. 6. Same as Fig. 5 for $h=0.5$, 0.8, 1, 2 from bottom to top.

$$C_{Z,R}(h=0,t) = \frac{1}{4}(\cos(\mu)^{N-2} - 1 + \{[\cos(\mu)^{N-2} - 1]^2 + [4\cos(\mu/2)^{N-2}\sin(\mu/2)]^2\}^{1/2}), \tag{18}$$

where, as previously, $\mu=4\lambda t/N$. The expression for $C_{Z,R}(h=0,t)$ given above is obtained by noting that the condition

$$2\rho_{22}^{(2)} < \sqrt{\rho_{11}^{(2)}\rho_{44}^{(2)}} + |\rho_{14}^{(2)}| \tag{19}$$

is always satisfied. Thus in the large-N limit, τ_Z is equal to 1 except for $\mu=0[2\pi]$ where $\tau_Z=0$ and, as expected, the concurrence vanishes for all μ. However, if one considers the rescaled concurrence, a close inspection of expression (19) shows that a periodic pulse also occurs for $\mu=0[2\pi]$ whose width becomes sharper and shaper as N increases and whose maximum height goes to 1 in the large-N limit.

At this stage, it is interesting to note that τ_Z and $C_{Z,R}$ are strongly correlated in the sense that, when the one-spin entanglement is large (and here maximum), the two-spin entanglement is small except for $\mu\simeq 0[2\pi]$. This is a relatively surprising result which is also encountered in other regimes (see below). Indeed, usually the trace operation destroys some correlations and one expects that the absence of two-spin entanglement might not be able to generate one-spin entanglement. Nevertheless, as discussed in Sec. III, this phenomenon is met for the $|\mathrm{GHZ}\rangle$ state, but here it is encountered for a nonstationary state which preserves this feature as time goes on.

(ii) For $\lambda=0$, the $|Z\rangle$ state is an eigenstate of H so that $\tau_Z(\lambda=0)=0$ and $C_Z(\lambda=0)=0$ for all time t. Contrarily to the $|X\rangle$ state, the limit $\lambda=0$ coincides with the high-field regime at finite λ. Indeed, as discussed in Ref. [34], the $|Z\rangle$ state is the ground state of H for $h>\lambda$ in the thermodynamical limit, so that $\tau_Z(h>\lambda)\simeq 0$ and $C_Z(h>\lambda)\simeq 0$.

However, the rescaled concurrence has a nontrivial behavior that can be captured due to its relation with the spin squeezing parameter [58]

$$\xi^2 = \frac{4(\Delta S_{\vec{n}_\perp})^2}{N}, \tag{20}$$

which measures the spin fluctuations of a correlated quantum state [58]. The subscript $\vec{n}_\perp$ refers to an axis perpendicular to the mean spin $\langle\vec{S}\rangle$ where the minimal value of the variance is obtained.

Indeed, as shown in Refs. [59,60], for any state belonging to the subspace $S=N/2$ and eigenstate of the operator $\Pi_i\sigma_z^i$, one has

$$\xi^2 = 1 - C_R, \tag{21}$$

provided the reduced density matrix elements of the state considered verify $|\rho_{14}^{(2)}| \geqslant \rho_{22}^{(2)}$. We have checked that actually this inequality is always satisfied for any h and for all the times under investigation.

(iii) The relation (21) thus allows us to deduce the rescaled concurrence using the frozen-spin approximation used in Ref. [49] to compute ξ^2 in two different regimes.

(a) For $h>\lambda$, as explained above, the $|Z\rangle$ state is the ground state of H in the infinite-N limit. So, even at finite N,

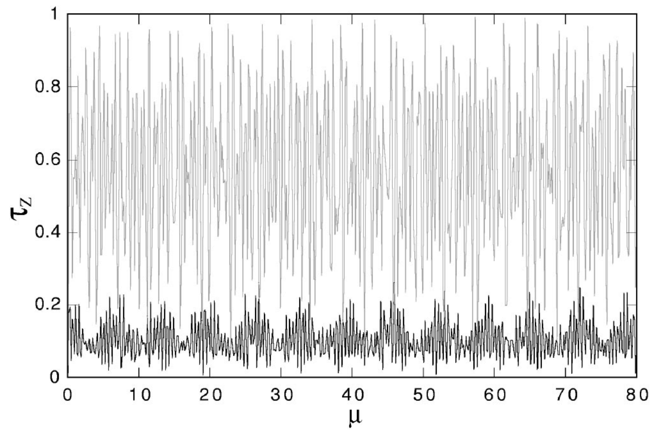

FIG. 7. Behavior of τ_Z as a function of $\mu=4\lambda t/N$ for $h=0.01$ (grey) and $h=0.9$ (black) ($\lambda=+1$ and $N=10^3$).

one expects $\langle S_z\rangle$ to be almost constant in this region. The so-called frozen-spin approximation precisely consists in replacing, in the Heisenberg equation, $S_z(t)$ by its initial value $N/2$. Then, following Ref. [49] and using Eq. (21), one gets an analytical expression for the rescaled concurrence,

$$C_{Z,R} = 1 - \left[\cos^2(\omega t) + \frac{w^2}{4h^2}\sin^2(\omega t)\right], \qquad (22)$$

with $\omega=2\sqrt{h(h-\lambda)}$.

(b) For $h<0$, the situation is, in fact, similar. Indeed, as shown in Ref. [36], the $|Z\rangle$ state is the ground state of $H(\lambda<0,h>0)$ in the thermodynamical limit. As detailed in Appendix A, this implies that it is the highest-energy state of $H(\lambda>0,h<0)$. Thus, the frozen-spin approximation can also be used in the region $(h<0)$ and, according to Ref. [49], one then obtains

$$C_{Z,R} = 1 - \left[\cos^2(\omega t) + \frac{4h^2}{w^2}\sin^2(\omega t)\right]. \qquad (23)$$

Of course, this approximation is more and more valid in these regions ($h<0$ and $h>\lambda$) when N increases. Conversely, at fixed N, it is safe for either $h\gg\lambda$ or $h\ll 0$.

The only region where the $|Z\rangle$ state is not an eigenstate of H in the thermodynamical limit is $0<h<\lambda$. We have plotted in Fig. 7 the behavior of τ_Z as a function of the rescaled dimensionless time $\mu=4\lambda t/N$ for different values of the magnetic field h in this range.

As explained above, $\tau_Z\simeq 0$ for $h<0$ and $h>\lambda$ since, there, $|Z\rangle$ is an eigenstate of H in the large-N limit. By contrast, for $h\in[0,\lambda]$, τ_Z is an oscillating function of μ with an average value that is nonvanishing as can be seen in Fig. 7. The time-averaged value of τ_Z for different N is shown in Fig. 8.

As can be seen, $\overline{\tau_Z}$ is a decreasing function of N at fixed h except for $h=0$ as discussed above. To determine its large-N behavior, we have computed $\overline{\tau_Z}$ for several h, as a function of N, up to $N=5000$. The results displayed in Fig. 9 do not allow us to extract an asymptotic value but it is likely that for $h\in[0,\lambda]$, $\lim_{N\to\infty}\overline{\tau_Z}\neq 0$.

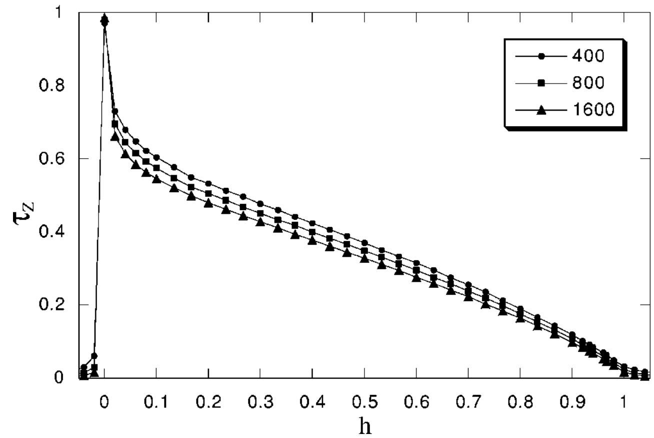

FIG. 8. Time-averaged value of τ_Z as a function of the magnetic field h for $N=400,800,1600$ ($\lambda=+1$).

As for the $|X\rangle$ state, we could have tried to reproduce this behavior by a classical analysis, but unfortunately, the $|Z\rangle$ state is a fixed point of the classical equations of motion (B8) and (B9). Thus, one must in this case use a real semiclassical treatment analogous to that presented in Ref. [41] which consists in averaging over classical trajectories near this fixed point. However, as shown in Fig. 7, τ_Z is a strongly oscillating function so that the approximation (15) is not valid and we did not compute the "semiclassical time-averaged one-tangle" for the $|Z\rangle$ state.

We now focus on the concurrence dynamics for the $|Z\rangle$ state, whose behavior is shown in Fig. 10 for $h=5\lambda$. As can be seen, the frozen-spin approximation is, in this case, in good agreement with the exact (numerical) results. For $h\in[0,\lambda]$, $C^*_{Z,R}$ is always negative so that $C_{Z,R}=0$. It is worth noting that there is once again an "anticorrelation" between the one-tangle and the rescaled concurrence since $\tau_X\neq 0$ when $C_{Z,R}=0$ for $h\in[0,\lambda]$, whereas for $h\in\,]-\infty,0]\cup[\lambda,\infty[$, one has $\tau_X=0$ and $C_{Z,R}\neq 0$. Indeed, in this latter region where $|Z\rangle$ becomes an eigenstate in the thermodynamical limit, one always has a nonvanishing rescaled concurrence as can be seen in Fig. 11 where we have displayed the time-averaged value of $C_{Z,R}$ as a function of h. At large $|h|$ the frozen-spin approximation allows us to extract the asymptotic behavior $\overline{C_{Z,R}}\sim|\lambda/h|$.

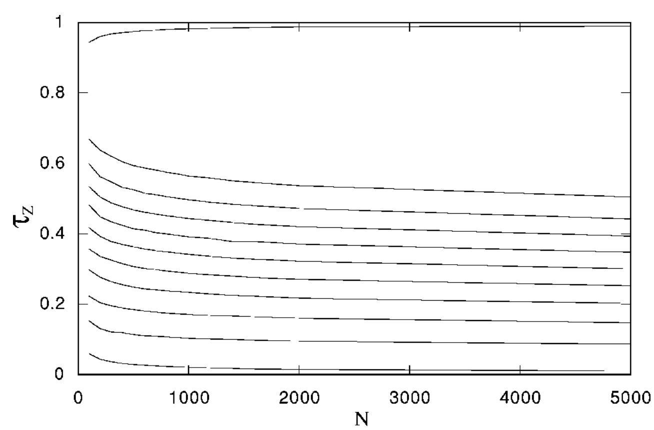

FIG. 9. Behavior of $\overline{\tau_Z}$ as a function of N for $h=0$ (top) to 1 (bottom) with a step $\Delta h=10^{-1}$ ($\lambda=+1$).

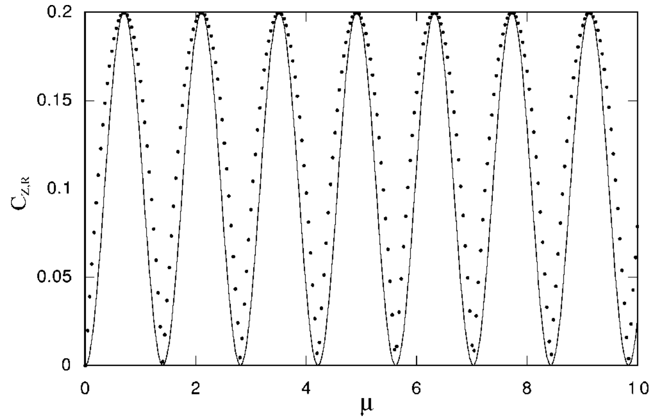

FIG. 10. Behavior of $C_{Z,R}$ as a function of $\mu=4\lambda t/N$ for $h=5$ ($\lambda=+1$ and $N=10^3$). Dots are obtained from the exact numerical diagonalizations and the solid line is computed with the frozen-spin approximation (22).

VI. CONCLUSION AND OUTLOOKS

We have analyzed the one-spin and two-spin entanglement dynamics for two different states. In the case of a state fully polarized in the x direction, we have found a nontrivial behavior of the one-tangle whose time-averaged value increases monotonically when the magnetic field increases whereas it has a vanishing concurrence for all h. By contrast, for an initial state fully polarized in the z direction, the one-tangle is nonvanishing only for $h\in[0,\lambda]$ where its concurrence vanishes. Apart from this region, the one-tangle vanishes in the thermodynamical limit (since $|Z\rangle$ is then an eigenstate of H) but the rescaled concurrence has a nontrivial time-averaged value which can be understood using the frozen-spin approximation introduced in Ref. [49].

Contrary to the ground-state entanglement, we did not find a nontrivial singularity at the critical point $h=\lambda$ but only some enhanced fluctuations near $h=\lambda/2$ for the $|X\rangle$ state. For the $|Z\rangle$ state, we have not detected any peculiarity at this point except that $\partial_h\overline{\tau_Z}$ seems to be minimum there whereas $\partial_h\overline{\tau_X}$ is maximum.

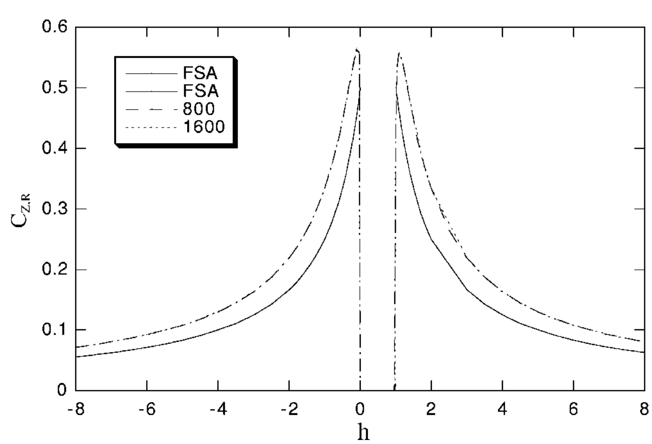

FIG. 11. Time-averaged value of $C_{Z,R}$ as a function of the magnetic field h for $N=800, 1600$ ($\lambda=+1$). The solid line corresponds to both branches ($h<0$ and $h>1$) of the frozen-spin approximation (FSA).

We wish to emphasize that some experiments may be possible to investigate these dynamical entanglement, especially the concurrence. Indeed, as explained in Sec. V C, the rescaled concurrence can be related to the spin squeezing parameter as established in Refs. [59,60]. Thus, the behavior of the C_R as a function of the field should, in principle, be measured for both the ground state and $|Z(t)\rangle$. Nevertheless, such an exciting perspective is of course conditioned by the possibility to measure the squeezing parameter. Bose-Einstein condensates are certainly the best candidates for such experiments since it has already been possible to measure the angular momentum in such systems [61].

ACKNOWLEDGMENTS

We would like thank B. Douçot, J. Dukelsky, R. Mosseri, and D. Mouhanna for fruitful discussions.

APPENDIX A: SPECTRUM SYMMETRIES AND THEIR IMPLICATIONS FOR THE DYNAMICS

Let us consider an eigenstate of the Hamiltonian H,

$$|\phi\rangle=\sum_{i=0}^{2^N-1}\alpha_i|i\rangle, \tag{A1}$$

such that

$$H(\lambda,h)|\phi\rangle=E|\phi\rangle. \tag{A2}$$

It is then straightforward to show that

$$|\varphi\rangle=\sum_{i=0}^{2^N-1}\alpha_{2^N-1-i}|i\rangle \tag{A3}$$

satisfies

$$H(-\lambda,+h)|\varphi\rangle=-E|\varphi\rangle, \tag{A4}$$

$$H(\lambda,-h)|\varphi\rangle=E|\varphi\rangle. \tag{A5}$$

Here, we have used a natural coding of the Hilbert space states where the number i (and its associated state $|i\rangle$) is in a one-to-one correspondence with its binary decomposition expressed in terms of $\uparrow$ (1) or $\downarrow$ (0) spins. These identities show that the spectrum of H is odd under the transformation $\lambda\rightarrow-\lambda$ and even under $h\rightarrow-h$. Moreover, they also imply that

$$H(-\lambda,-h)|\phi\rangle=-E|\phi\rangle, \tag{A6}$$

so that $H(+\lambda,+h)$ and $H(-\lambda,-h)$ have the same eigenstates but with opposite eigenenergies.

Let us now consider a state $|\psi\rangle$ whose spectral decomposition on the eigenstates of H reads

$$|\psi\rangle=\sum_{j=0}^{2^N-1}a_j|\phi_j\rangle, \tag{A7}$$

where all the a_i's are real numbers, and an observable A satisfying

$$\langle \phi_{j'}|A|\phi_j\rangle = \langle \phi_j|A|\phi_{j'}\rangle, \tag{A8}$$

for all (j,j'). Then from Eq. (A6) one has

$$\langle \psi_{+,+}(t)|A|\psi_{+,+}(t)\rangle = \langle \psi_{-,-}(t)|A|\psi_{-,-}(t)\rangle, \tag{A9}$$

where $|\psi_{\pm,\pm}(t)\rangle = e^{-iH(\pm\lambda,\pm h)t}|\psi\rangle$. In addition, it is clear that the density matrix matrices $\rho_{+,+}$ and $\rho_{-,-}$ are identical.

APPENDIX B: SEMICLASSICAL APPROACH

The Heisenberg equations for the spin operators are given by

$$\dot{S}_x = 2hS_y, \tag{B1}$$

$$\dot{S}_y = -2hS_x + \frac{2\lambda}{N}(S_zS_x + S_xS_z), \tag{B2}$$

$$\dot{S}_z = -\frac{2\lambda}{N}(S_yS_x + S_xS_y). \tag{B3}$$

These equations cannot be solved exactly for any (λ,h) and any initial conditions. To investigate the spin dynamics, we follow Milburn *et al.* [54] and consider the semiclassical dynamics (mean-field approximation) associated with these equations by considering the "double-well" parametrization (Schwinger-like) for the spin variables which reads

$$s_x = \frac{N}{2}(|b_2|^2 - |b_1|^2), \tag{B4}$$

$$s_y = -\frac{iN}{2}(b_1^* b_2 - b_1 b_2^*), \tag{B5}$$

$$s_z = \frac{N}{2}(b_1^* b_2 + b_1 b_2^*). \tag{B6}$$

The complex variables b_1 and b_2 satisfy the constraint $|b_1|^2 + |b_2|^2 = 1$ and obey

$$\dot{b}_j = ihb_{3-j} + 2i\lambda|b_j|^2 b_j, \tag{B7}$$

for $j=1,2$. This type of equation has been studied in detail by Eilbeck *et al.* so that we only sketch here the main lines of the solutions and refer the reader to Ref. [57] for details. Setting $b_j = a_j e^{i\theta_j}$ (for $j=1,2$) and $\theta=\theta_1-\theta_2$, the latter nonlinear equation system (B7) is rewritten as

$$\dot{a}_1 = h(1-a_1^2)^{1/2}\sin\theta, \tag{B8}$$

$$\dot{\theta} = 2(a_1^2-1)\left(2\lambda - \frac{h\cos\theta}{a_1(1-a_1^2)^{1/2}}\right). \tag{B9}$$

Then, using the conservation of energy,

$$E(a_1,\theta) = -\lambda[1-2a_1^2(1-a_1^2)] - 2ha_1(1-a_1^2)^{1/2}\cos\theta, \tag{B10}$$

$$= \frac{1}{N}\left[H(a_1,\theta) - \lambda/2 - \frac{\lambda N}{2}\right], \tag{B11}$$

we can eliminate θ to get a closed equation for a_1.

From now on, we consider the initial conditions $a_1(0)=1$ and $\theta(0)=0$ which describe a state polarized in the $-x$ direction—i.e., the classical counterpart of the $|-X\rangle$ state. This state is not the one considered in Sec. V B since it lies in the opposite direction, but for clarity, we have used the same notation as in Refs. [54,57]. One thus has

$$E(a_1,\theta) = -\lambda, \tag{B12}$$

so that from the energy conservation (B10), one gets

$$\cos\theta = \frac{\lambda}{h}a_1(1-a_1^2)^{1/2}. \tag{B13}$$

Next, using Eq. (B8) and setting $a_1^2=(1+y)/2$, it is straightforward to show that

$$\left(\frac{\dot{y}}{2h}\right)^2 = 1-k^2+(2k^2-1)y^2-k^2y^4, \tag{B14}$$

where $k=\lambda/(2h)$. The solution of this equation is the Jacobi elliptic function

$$y(t) = \mathrm{cn}(2ht|k^2), \tag{B15}$$

which yields

$$S_x(t) = \frac{N}{2}(1-2a_1^2) = -\frac{N}{2}\mathrm{cn}(2ht|k^2), \tag{B16}$$

$$S_y(t) = -Na_1\dot{a}_1/h = \frac{N}{2}\mathrm{dn}(2ht|k^2)\mathrm{sn}(2ht|k^2), \tag{B17}$$

$$S_z(t) = \frac{N\lambda}{h}a_1^2(1-a_1)^2 = \frac{N\lambda}{4h}\mathrm{sn}^2(2ht|k^2). \tag{B18}$$

Finally, since we are not interested in the $|-X\rangle$ but in the $|X\rangle$ state, we just have to change the sign correctly and we get the expression given in Sec. V B.

APPENDIX C: ONE-SPIN AND TWO-SPIN REDUCED DENSITY MATRICES OF FULLY SYMMETRIC STATES

Let us consider a state

$$|\psi\rangle = \sum_{M=-N/2}^{+N/2}\alpha_M|N/2,M\rangle, \tag{C1}$$

where $\{|S,M\rangle\}$ is an eigenbasis of $\mathbf{S}^2$ and S_z, and its density matrix $\rho=|\psi\rangle\langle\psi|$. Here, we restrict our discussion to states belonging to the maximum spin sector $S=N/2$ which are relevant for BEC.

In this subspace, all states are invariant under the permutation group $\mathcal{S}_N$, so that one can easily compute the matrix elements of the reduced density matrices $\rho_i^{(1)}$ and $\rho_{i,j}^{(2)}$. Note that the permutation symmetry implies that $\rho_i^{(1)}$ does not depend on i and that $\rho_{i,j}^{(2)}$ does not depend on i and j, so that we omit these indices in the following.

As is well known, the one-spin reduced density matrix is easily expressed in terms of the one-spin correlation functions or, more precisely, in terms of the $\langle\sigma_\alpha\rangle$'s. In the eigenbasis $\{|\uparrow\rangle, |\downarrow\rangle\}$ of σ_z, a straightforward calculation gives

$$\rho_{11}^{(1)} = \frac{1}{2} + \sum_M |\alpha_M|^2 \frac{M}{N}, \tag{C2}$$

$$\rho_{22}^{(1)} = \frac{1}{2} - \sum_M |\alpha_M|^2 \frac{M}{N}, \tag{C3}$$

$$\rho_{12}^{(1)} = \sum_M \alpha_M \alpha_{M+1}^* \frac{\sqrt{(N-2M+2)(N+2M)}}{2N}, \tag{C4}$$

with $\rho_{ij}^{(1)} = \rho_{ji}^{(1)*}$.

The two-spin reduced density matrix can also be easily expressed in terms of the two-spin correlation functions (see Ref. [60]). In the eigenbasis $\{|\uparrow\uparrow\rangle, |\uparrow\downarrow\rangle, |\downarrow\uparrow\rangle, |\downarrow\downarrow\rangle\}$, one has

$$\rho_{11}^{(2)} = \sum_M |\alpha_M|^2 \frac{(N+2M)(N+2M-2)}{4N(N-1)}, \tag{C5}$$

$$\rho_{12}^{(2)} = \sum_M \alpha_M \alpha_{M+1}^* (N+2M-2) \frac{\sqrt{(N-2M+2)(N+2M)}}{4N(N-1)}, \tag{C6}$$

$$\rho_{14}^{(2)} = \sum_M \alpha_M \alpha_{M+2}^* \sqrt{(N+2M)(N+2M-2)} \times \frac{\sqrt{(N-2M+2)(N-2M+4)}}{4N(N-1)}, \tag{C7}$$

$$\rho_{24}^{(2)} = \sum_M \alpha_M \alpha_{M+1}^* (N-2M) \frac{\sqrt{(N-2M+2)(N+2M)}}{4N(N-1)}, \tag{C8}$$

$$\rho_{22}^{(2)} = \sum_M |\alpha_M|^2 \frac{(N-2M)(N+2M)}{4N(N-1)}, \tag{C9}$$

$$\rho_{44}^{(2)} = \sum_M |\alpha_M|^2 \frac{(N-2M)(N-2M-2)}{4N(N-1)}, \tag{C10}$$

with $\rho_{13}^{(2)} = \rho_{12}^{(2)}$, $\rho_{23}^{(2)} = \rho_{33}^{(2)} = \rho_{22}^{(2)}$, $\rho_{34}^{(2)} = \rho_{24}^{(2)}$, and $\rho_{ij}^{(2)} = \rho_{ji}^{(2)*}$.

[1] T. J. Osborne and M. A. Nielsen, Phys. Rev. A **66**, 032110 (2002).
[2] A. Osterloh, L. Amico, G. Falci, and R. Fazio, Nature (London) **416**, 608 (2002).
[3] G. Vidal, J. I. Latorre, E. Rico, and A. Kitaev, Phys. Rev. Lett. **90**, 227902 (2003).
[4] J. I. Latorre, E. Rico, and G. Vidal, Quantum Inf. Comput. **4**, 48 (2004).
[5] S. J. Gu, H. Q. Lin, and Y. Q. Li, Phys. Rev. A **68**, 042330 (2003).
[6] V. E. Korepin, Phys. Rev. Lett. **92**, 096402 (2004).
[7] U. Glaser, H. Büttner, and H. Fehske, Phys. Rev. A **68**, 032318 (2003).
[8] I. Bose and E. Chattopadhyay, Phys. Rev. A **66**, 062320 (2002).
[9] O. F. Syljuasen, Phys. Rev. A **68**, 060301 (2003).
[10] O. F. Syljuasen, Phys. Lett. A **322**, 25 (2004).
[11] F. Verstraete, M. Popp, and J. I. Cirac, Phys. Rev. Lett. **92**, 027901 (2004).
[12] F. Verstraete, M. A. Martin-Delgado, and J. I. Cirac, Phys. Rev. Lett. **92**, 087201 (2004).
[13] B. Q. Jin and V. E. Korepin, Phys. Rev. A **69**, 062314 (2004).
[14] T. Roscilde *et al.*, Phys. Rev. Lett. **93**, 167203 (2004).
[15] T. Stauber and F. Guinea, Phys. Rev. A **70**, 022313 (2004).
[16] F. C. Alcaraz, A. Saguia, and M. S. Sarandy, Phys. Rev. A **70**, 032333 (2004).
[17] O. Osenda, Z. Huang, and S. Kais, Phys. Rev. A **67**, 062321 (2003).
[18] C. Wellard and R. Orus, e-print quant-phys/0401144.
[19] N. Lambert, C. Emary, and T. Brandes, Phys. Rev. Lett. **92**, 073602 (2004).
[20] N. Lambert, C. Emary, and T. Brandes, e-print quant-phys/0405109.
[21] P. Stelmachovic and V. Buzek, Phys. Rev. A **70**, 032313 (2004).
[22] H. Fan, V. Korepin, and V. Roychowdhury, e-print quant-phys/0406067.
[23] S. J. Gu, Y. Q. Li, and H. Q. Lin, e-print quant-ph/0310030.
[24] H. Li, X. Wang, and Y. Li, e-print quant-ph/0403178.
[25] Y. Shi, J. Phys. A **37**, 6807 (2004).
[26] H. J. Lipkin, N. Meshkov, and A. J. Glick, Nucl. Phys. **62**, 188 (1965).
[27] N. Meshkov, A. J. Glick, and H. J. Lipkin, Nucl. Phys. **62**, 199 (1965).
[28] A. J. Glick, H. J. Lipkin, and N. Meshkov, Nucl. Phys. **62**, 211 (1965).
[29] R. Botet, R. Jullien, and P. Pfeuty, Phys. Rev. Lett. **49**, 478 (1982).
[30] R. Botet and R. Jullien, Phys. Rev. B **28**, 3955 (1983).
[31] J. I. Cirac, M. Lewenstein, K. Mølmer, and P. Zoller, Phys. Rev. A **57**, 1208 (1998).
[32] J. Dukelsky, S. Pittel, and G. Sierra, Rev. Mod. Phys. **76**, 643 (2004).
[33] J. Links, H.-Q. Zhou, R. H. McKenzie, and M. D. Gould, J. Phys. A **36**, R63 (2003).
[34] J. Vidal, G. Palacios, and R. Mosseri, Phys. Rev. A **69**, 022107 (2004).
[35] S. Dusuel and J. Vidal, Phys. Rev. Lett. **93**, 237204 (2004).
[36] J. Vidal, R. Mosseri, and J. Dukelsky, Phys. Rev. A **69**, 054101 (2004).
[37] W. K. Wootters, Phys. Rev. Lett. **80**, 2245 (1998).
[38] L. Amico *et al.*, Phys. Rev. A **69**, 022304 (2004).

[39] S. Montangero, G. Benenti, and R. Fazio, Phys. Rev. Lett. **91**, 187901 (2003).
[40] A. P. Hines, R. H. McKenzie, and G. J. Milburn, Phys. Rev. A **67**, 013609 (2003).
[41] A. Micheli, D. Jaksch, J. I. Cirac, and P. Zoller, Phys. Rev. A **67**, 013607 (2003).
[42] H. Ng, C. K. Law, and P. T. Leung, Phys. Rev. A **68**, 013604 (2003).
[43] H. Ng and P. T. Leung, e-print quant-phys/0405117.
[44] A. Einstein, B. Podolsky, and N. Rosen, Phys. Rev. **47**, 777 (1935).
[45] V. Coffman, J. Kundu, and W. K. Wootters, Phys. Rev. A **61**, 052306 (2000).
[46] D. M. Greenberger, M. A. Horne, and A. Zeilinger, in *Bell's Theorem, Quantum Theory, and Conceptions of the Universe*, edited by M. Kafatos (Kluwer Academic, Dordrecht, 1989).
[47] J. I. Latorre, R. Orús, E. Rico, and J. Vidal, e-print cond-mat/0409611.
[48] A. P. Hines, G. J. Milburn, and R. H. McKenzie, e-print quant-ph/0308165.
[49] C. K. Law, H. T. Ng, and P. T. Leung, Phys. Rev. A **63**, 055601 (2001).
[50] D. Gordon and C. M. Savage, Phys. Rev. A **59**, 4623 (1999).
[51] M. Zhang, K. Helmerson, and L. You, Phys. Rev. A **68**, 043622 (2003).
[52] G. Kalosakas, A. R. Bishop, and V. M. Kenkre, J. Phys. B **36**, 3233 (2003).
[53] G. Kalosakas, A. R. Bishop, and V. M. Kenkre, Phys. Rev. A **68**, 023602 (2003).
[54] G. J. Milburn, J. Corney, E. M. Wright, and D. F. Walls, Phys. Rev. A **55**, 4318 (1997).
[55] X. Wang and K. Mølmer, Eur. Phys. J. D **18**, 385 (2002).
[56] L. Bernstein, J. C. Eilbeck, and A. C. Scott, Nonlinearity **3**, 293 (1990).
[57] J. C. Eilbeck, P. S. Lomdahl, and A. C. Scott, Physica D **16**, 318 (1985).
[58] M. Kitagawa and M. Ueda, Phys. Rev. A **47**, 5138 (1993).
[59] A. Messikh, Z. Ficekh, and M. R. B. Wahiddin, J. Opt. B: Quantum Semiclassical Opt. **5**, L1 (2003).
[60] X. Wang and B. C. Sanders, Phys. Rev. A **68**, 012101 (2003).
[61] F. Chevy, K. W. Madison, and J. Dalibard, Phys. Rev. Lett. **85**, 2223 (2000).